Journal of Solid State Chemistry 182 (2009) 2756–2761

Contents lists available at ScienceDirect

Journal of Solid State Chemistry

journal homepage: www.elsevier.com/locate/jssc

Compositional dependence of the nonlinear refractive index of new germanium-based chalcogenide glasses

L. Petit [a,*], N. Carlie [a], H. Chen [a], S. Gaylord [a], J. Massera [a], G. Boudebs [b], J. Hu [c], A. Agarwal [c], L. Kimerling [c], K. Richardson [a]

[a] School of Materials Science and Engineering, Clemson University, Clemson, SC 29634, USA
[b] Laboratoire des Proprietes Optiques des Materiaux et Applications, UMR CNRS 6163, Universite d'Angers, 2 Boulevard Lavoisier, 49045 Angers Cedex 01, France
[c] Microphotonics Center, Massachusetts Institute of Technology, Cambridge, MA 02139, USA

ARTICLE INFO

Article history:
Received 19 May 2009
Received in revised form
13 July 2009
Accepted 18 July 2009
Available online 25 July 2009

Keywords:
Chalcogenide glass
Nonlinear refractive index
Raman spectroscopy

ABSTRACT

In this paper, we report results of n_2 measurements of new chalcogenide glasses in the Ge–Sb–S–Se system using a modified Z-Scan technique. Measurements were made with picosecond pulses emitted by a 10 Hz Q-switched mode-locked Nd-YAG laser at 1064 nm under conditions suitable to characterize ultrafast nonlinearities. The nonlinear index increases up to 500 times the n_2 of fused silica with an increase in the Ge/Se ratio and a decrease with an increase of the Ge/Sb ratio. We confirmed, using Raman spectroscopy, that the nonlinear refractive index depends on the number of Ge–S(Se) and Sb–S(Se) bonds in the glass network. Sulfide glasses were shown to have a nonlinear FOM near or <1, at 1064 nm.

1. Introduction

Chalcogenide glasses (ChGs) have received increased interest due to their high linear and nonlinear indices of refraction and good transmittance into the infrared region. These materials are seen as potential candidates for infrared optics, photonic devices, reversible optical recording media, all-optical switching, and inorganic photoresists [1]. The nonlinear properties of glasses in the As–Se–S system have been largely studied [2]. The introduction of selenium to the As–S system increases n_2 up to 400 times the n_2 of fused silica [3] while still maintaining low nonlinear absorption (β) and a figure of merit [4] <1. High Se content within the As–S/Se binary and ternary systems has been shown to further increase $n_2/n_{2(SiO_2)}$ but at the expense of a marked increase in linear and nonlinear absorption [5]. The nonlinear properties of chalcogenide glasses in the systems: Ge–S(Se), Ge–As–S(Se), As–S–Se, and Ge–As–S–Se, have been also extensively investigated [6–9]. Recently, the effects of halogen or halide addition on glass-forming ability, structural organization or band-gap energy have also been studied in As–S, Ge–S, Sb–S and Ge–Ga–S based chalcogenide glasses [2,10–13]. It was found that the introduction of halogen generally decreases the band-gap wavelength towards the blue region of the visible spectrum due to the electronegativity of the halogen atoms reducing the electron delocalization in the glass network, and consequently, decreasing the nonlinear refractive index of chalcogenide glasses [10].

Despite the extensive work in this area in the past decade, the origin of the nonlinearity of glass in general and chalcogenide glasses in particular, is still largely unclear. Cardinal et al. [3] showed that the large n_2 for glasses in the As–S–Se systems with small As/(S+Se) molar ratios was correlated with the presence of covalent, homopolar Se–Se bonds in the glass structure as identified by Raman spectroscopy; in the equimolar chalcogen contributions, n_2 could not be attributed to any red shift in the absorption edge or to a resonant effect, unlike that seen in high chalcogen content in binary As_2Se_3 materials [6]. Subsequent to this, Harbold et al. [14] showed that n_2 is not solely dependent on the lone pair electron concentration associated with the chalcogen and group V species, but also on resonant enhancement of the optical band gap, as defined by a normalized photon energy which takes into account incident energy of the wavelength of use and the material's band-gap energy [14]. Recently, Sanghera et al. related the nonlinear index to the normalized photon energy and provided a predictive capability for the nonlinear index, over a large wavelength range, if the band gap of the glass is known [15].

Recent studies in our group have further compared the relationship of glass composition and structure, refractive index (linear and nonlinear) to other high intensity effects such as Raman Gain. Our results in heavy metal oxide glasses [16–18] as well as in diverse chalcogenide glass systems [19] illustrates the ability to tailor material structure and optical response (linear and nonlinear), along with laser damage resistance (critical for use of

* Corresponding author.
E-mail address: lpetit@clemson.edu (L. Petit).

0022-4596/$ - see front matter © 2009 Elsevier Inc. All rights reserved.
doi:10.1016/j.jssc.2009.07.027

chalcogenides in high intensity applications) through selective choice of glass constituents. In a recent study of the glasses with the composition $Ge_{23}Sb_7S_{70-x}Se_x$, [20], we further showed using X-ray photoelectron spectroscopy (XPS) in conjunction with n_2 measurements that an increase of Ge–Se bond from 2×10^{21} to $8\times10^{21}/cm^3$ leads to an increase of the n_2 from 2×10^{-18} to 10×10^{-18} m^2/W indicating that n_2 depends on the number of heteropolar and homopolar bonds forming the glass network. To confirm this hypothesis, new glasses in the same Ge–Sb–S(Se) systems have been prepared with varying Ge/chalcogen [S,Se] and Ge/Sb ratios to evaluate the specific impact of constituents and their structural role, on resulting nonlinear material response.

In this paper, we report the physical, thermal and optical properties of the new glasses and present corresponding evaluation of their structure via Raman spectroscopy, thus correlating structural changes to physical property evolution with constituents. The nonlinear refractive index and absorption of the new glasses are presented and we interpret the variation in behavior to chemical composition and structure of the glass network.

2. Experimental

Glasses in the Ge–Sb–S and Ge–Sb–Se systems are prepared from high purity elements (Ge Aldrich 99.999%, Sb Alpha 99.9%, S and Se Cerac 99.999%). Starting materials are weighed and batched into quartz ampoules inside a nitrogen-purged glove box and sealed under vacuum using an oxygen gas torch. Prior to sealing and melting, the ampoule and batch are pre-heated at 100 °C for 4 h to remove surface moisture from the quartz ampoule and the batch raw materials. After sealing, the ampoule is heated for 24 h between 900 and 975 °C, depending on the glass composition. Once homogenized, the melt-containing ampoule is air–quenched to room temperature. To avoid fracture of the tube and glass ingot, the ampoules are subsequently returned to the furnace for annealing for 15 h at 40 °C below the glass transition temperature, T_g. The same procedure is used for selenium-substituted compositions. The glass samples are then cut, optically polished and visually inspected for defects that reduce optical quality needed for the Z-scan measurements.

The glass transition temperature (T_g) is determined by differential scanning calorimetry (DSC) at a heating rate of 10 °C/min from 50 to 450 °C using a commercial DSC apparatus (TA Instrument Inc.). The measurements are carried out in a hermetically sealed aluminum pan.

The density of the resulting bulk glass materials is measured by Archimedes' principle using diethylphthalate at room temperature. The measurement accuracy is better than 0.3%.

Spectroscopic ellipsometry is used to examine the refractive index of the glasses using a J.A. Woollam model M-44 spectroscopic ellipsometer which incorporates a variable angle stage allowing adjustment of the incident angle. The instrument operates on a rotating polarizer principle, in which the polarization of incoming light is varied, and reflected intensity is recorded with a grating coupled CCD over a wavelength range of 600–1100 nm. Multiple measurements and subsequent curve fitting allowed a calculation of index variation with wavelength with a final error of approximately ±0.05. This technique allowed relative comparison of bulk glass refractive indices as a function of composition.

Absorption spectra of the investigated glasses are obtained at room temperature using a dual beam UV–Vis–NIR Perkin Elmer Lambda 900 spectrophotometer from 300 to 1500 nm.

The Raman spectra are recorded at room temperature, in backscattering geometry, using a Kaiser Hololab 5000R Raman spectrometer with Raman microprobe attachment (typical resolution of 2–3 cm^{-1}). The system consists of a holographic notch filter for Rayleigh rejection, a microscope equipped with $10\times$, $50\times$ and $100\times$ objectives (the latter allowing a spatial resolution of $<2\,\mu m$), and a CCD detector. A 785 nm semiconductor laser (Invictus 785, Kaiser Optical Systems Inc.) was used for excitation with incident power of around 2 mW. The use of a 785 nm source with a low power and short data collection time was deemed essential to our study to avoid photostructural changes which the laser beam may induce in the samples.

The nonlinear refractive index of the glasses is measured using the Z-scan method [21]. Excitation is provided by a Nd:YAG laser delivering linearly polarized 15 ps single pulses at $\lambda = 1064$ nm with 10 Hz repetition rate. Other experimental parameters in the classical Z-scan method include: f (focal length of the focusing lens) = 20 cm; d (distance from the beam waist plane to the camera) = 26 cm. The beam waist at the focal plane is $\omega_0 = 30\,\mu m$ giving a Rayleigh range $z_0 = \pi\omega_0^2/\lambda \approx 2.6$ mm. This value is larger than the sample thickness (typically 1 mm). The photodetector is a 1000×10^{-18} pixels cooled camera (Hamamatsu C4880) with fixed linear gain. The camera pixels have 4095 gray levels and each pixel is $12\times12\,\mu m^2$. Two sets of acquisitions (in the linear and the nonlinear regime) are carried out for the measurement to correct for inhomogenities and surface imperfections in the sample. Open and closed Z-scan normalized transmittances are numerically processed from the acquired images by integrating over all the pixels in the first case and over a circular numerical filter (with radius equal to 1 mm) in the second case.

3. Results and discussion

Recently, we showed that with a progressive replacement of S by Se in the Ge–Sb–S glass network, the non-resonant n_2 increases from 50 up to 350 times the value for fused silica [20]. Contrary to results seen in other As-based chalcogenide glass systems [5], these results were not seen to be simply related to the formation of homopolar Se–Se bonds and the associated increase in lone pair electron (LPE) concentration. Using XPS, we postulated that the increase of nonlinear refractive index in Ge–Sb–sulfo-selenide glasses may be attributed to the increase of Ge–Se and Sb–Se bonds in the glass network [20]. To validate more precisely this proposed interpretation observed for the glasses previously measured, we have expanded our study to systematically vary the types and number of Ge-chalcogen and Ge/Sb bonds in the glass network. With such analysis, the role of bond type, the chalcogen content and thus the LPE concentration on the resulting nonlinear optical material properties could be confirmed.

Table 1 summarizes the composition of the investigated glasses including the glass transition temperature (T_g), density, molar volume, the number of the lone pair electron (LPE), the normalized photon energy ($h\nu/E_{gap}$) and the glass' linear and nonlinear refractive index at 1064 nm. The lone pair electron concentration has been estimated assuming one electronic lone pair per Sb ion, two per S and Se ion, and no pairs per Ge ion. The number of ions has been calculated using the density and the molar weight of the glasses. The large bars seen for the reported index (n) and n_2 data are related to within-sample measurement variation due to poor surface quality of the glass samples. While care has been taken during polishing, Se-containing glasses are softer than Se-free compositions and thus are especially susceptible to scratching. Note that the n_2 measured in this study are in agreement with those reported by [22,23]. In agreement with [24,25], we see that the nonlinearity is determined completely by E_g. Both n_2 and β are strongly dependent upon E_g as $n_2 \propto 1/E_g^4$ and $\beta \propto 1/E_g^3$.

Table 1
Glass transition temperature, density, linear refractive index at 1064 nm and nonlinear characteristics measured by Z-Scan technique at $\lambda = 1064$ nm of the investigated glasses.

Glass composition	Ge/Sb ratio	Ge/Se ratio	Number of lone pair electron/cm^3	T_g (°C) (±5 °C)	Density (g/cm^3) (±0.02)	Molar volume (cm^3/mol)	n at 1064 nm (±0.05)	n_2 (10^{-18} m^2/W)	n_2/n_{silica}	β (cm/GW)	λ_{gap} (nm)[a]	F	E_{gap} (eV)	$h\nu/E_{gap}$
$Ge_{16}Sb_{14}S_{70}$	1.14	0.23	5.88E22	262	3.24	15.77	2.31	2.1±0.6	70	<0.1	580	<1.0	2.1	0.55
$Ge_{23}Sb_7S_{70}$ [26]	3.29	0.33	5.46E22	311	2.94	16.21	2.25	1.7±0.2	55	<0.1	530	<1.3	2.3	0.50
$Ge_{31}Sb_9S_{60}$	3.44	0.52	4.61E22	347	3.13	16.84	2.35	2.6±0.7	87	<0.1	675	<0.8	1.8	0.63
$Ge_{16}Sb_{14}Se_{70}$	1.14	0.23	5.18E22	214	4.69	17.90	2.68	15±5	500	3.4±0.7	804	4.8	1.5	0.76
$Ge_{13}Sb_7Se_{80}$	1.86	0.16	5.42E22	151	4.37	18.56	2.64	7.2±0.3	240	1.6±0.2	737	4.7	1.7	0.69
$Ge_{23}Sb_7Se_{70}$ [20]	3.29	0.33	5E22	246	4.55	17.69	2.62	10.3±1.5	343	2.4	745	5	1.7	0.70
$Ge_{28}Sb_7Se_{65}$	4.00	0.43	4.74E22	287	4.61	17.39	2.59	11.5±3	383	4.9±0.6	773	9.1	1.6	0.73
$Ge_{35}Sb_7Se_{58}$	5.00	0.60	4.64E22	299	5.00	15.95	2.58	9±2.7	367	3.3±0.5	777	7.8	1.6	0.73

The n_2 data of the selenide glasses have large error bars. This is attributed to the surface quality of the glasses which is not optimum.

[a] λ_{gap}, the band gap wavelength defined as the wavelength for which the linear absorption coefficient α is 10 cm^{-1}. n_2 is the nonlinear refractive index, β the nonlinear absorption and F the figure of merit at 1064 nm.

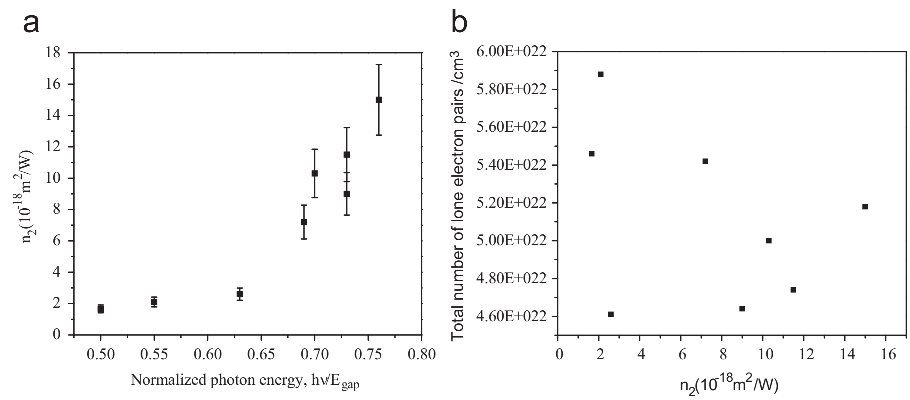

Fig. 1. Variation of n_2 at 1064 nm wavelength (a) as a function of normalized photon energy in the Ge–Sb–S–Se system and (b) as a function of the number of lone electron pairs.

Figs. 1a and b show the variation of n_2 as a function of normalized photon energy ($h\nu/E_{gap}$) and lone pair electron concentration (per cc of glass), respectively. It can be clearly seen that n_2 for both sulfide and selenide compositions increases with an increase of normalized photon energy, regardless of chalcogen type, but does not depend on the concentration of lone pair electron. The findings here, shown for a broad composition space within the ternary systems studied, are in agreement with data for the two compositions of our previous studies [20,26]. Additionally, it agrees with the findings of Harbold et al who have shown that n_2 is not solely dependent on the lone electron pair concentration but also on the energy gap which depends on the composition and glass constituents [14].

To be considered as a good candidate for ultra fast optical switch in an optical fiber configuration with a peak power of 1 W and an attenuation of 0.5 dB/m, candidate glasses must have a high nonlinear refractive index (nominally 400 times higher than that of silica or better) and a small value of β. The evaluation of the figure of merit (FOM), F, of the investigated glasses at 1064 nm listed in Table 1 was determined using the following equation:

$$F = \frac{2\beta\lambda}{n_2}$$

is listed in Table 1 [4].

The FOM of the sulfide glasses leads to values which are lower than 1 whereas it is higher than 1 for the selenide glasses. Quemard et al. [27] have measured the nonlinear refractive index of $As_{40}Se_{60}$ and $Ge_{20}As_{40}Se_{40}$ glasses at 1064 nm and also at 1430 nm. They have demonstrated that the value of the FOM of these glasses is higher than 1 at 1064 nm but <1 at 1430 nm. Compared to these results, we might also expect a similar diminution of the nonlinear absorption inducing a FOM <1 in Se compositions at 1430 nm and a more significant decrease of the FOM at around 1550 nm which is the telecommunication wavelength.

In order to confirm which of the primary physical properties dominates the origins of the optical nonlinearity in these glasses, the effect of composition on the physical, structural, linear, and nonlinear optical properties of the glasses has been made. For the glasses in the Ge–Sb–S system, when the Ge/Sb ratio decreases for a fixed sulfur content (70 at% S), a decrease in T_g occurs accompanied by a density increase and a red-shift in the absorption band gap. This band-gap position shift is shown in Fig. 2a. These variations are in agreement with our previous study [28]. We have demonstrated that the progressive introduction of Sb_2S_3 in the glass system $(1-x)GeS_{2-x}Sb_2S_3$ decreases the number of GeS_4 units in the glass network resulting in the dramatic decrease of the glass transition temperature and of the Vicker's microhardness and in an increase of the density and the linear refractive index. Similar behavior was observed for the glasses of composition $Ge_{0.23}Sb_yS_{0.77-y}$ with an increase of y [28]. The changes in the physical properties can be attributed to a decrease in the number of GeS_4 units in the glass network as depicted in Fig. 2b which shows the Raman spectra of the glasses evaluated in

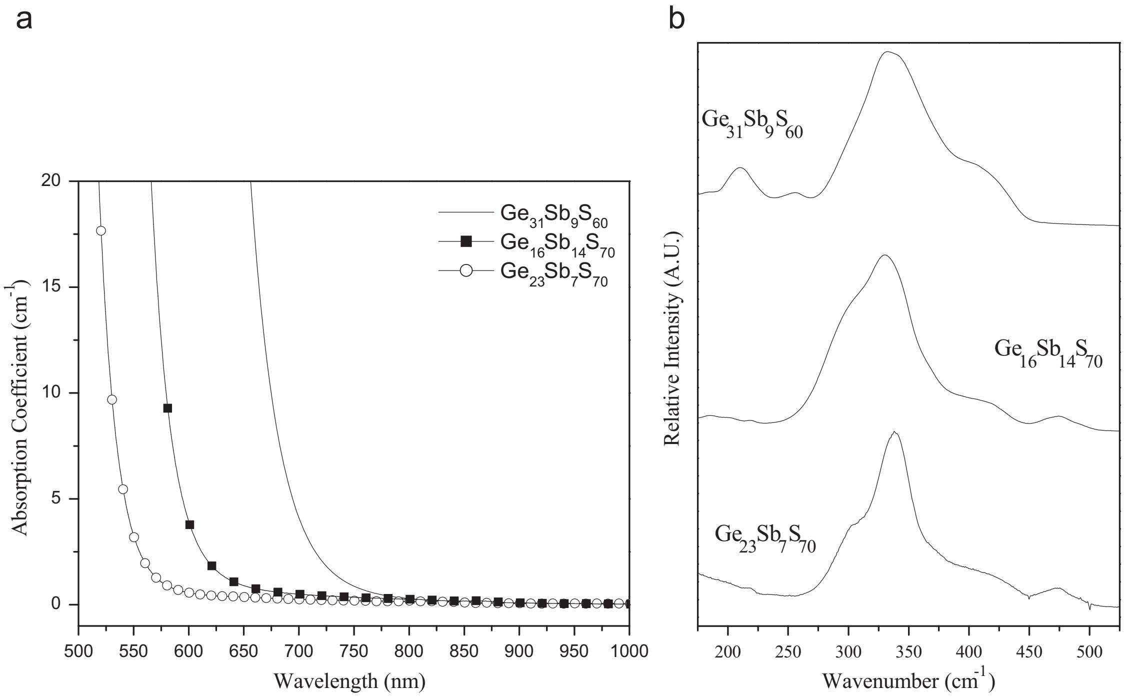

Fig. 2. (a) Absorption and (b) Raman spectra of the sulfide glasses.

this study. The Raman spectra of the glasses present a broad main band in the range of 300–425 cm^{-1} with bands of low amplitude in the 450–550 cm^{-1} range. In agreement with previous studies in the same ternary composition space, the bands at 330 and 340 cm^{-1} correspond to the A_1 mode of isolated GeS_4 [29] and corner-sharing $GeS_{4/2}$ [30] tetrahedral units, respectively. The shoulder at higher wavenumbers is composed of three bands near 375, 410, and 425 cm^{-1}. The bands near 375 and 410 cm^{-1} have been attributed, respectively, to the T_2 mode of edge-sharing $Ge_2S_4S_{4/2}$ bi-tetrahedra and the T_2 mode of corner-sharing $GeS_{4/2}$ while the band at 425 cm^{-1} is related to vibrations of two tetrahedra connected through one bridging sulfur atom, as in $S_3Ge–S–GeS_3$ [30]. The shoulder at around 300 cm^{-1} has been assigned to the E modes of $SbS_{3/2}$ pyramids [31]. The band near 475 cm^{-1} may be related to the A_1 vibration mode of sulfur S_8 rings, while the band at 490 cm^{-1} has been attributed to the A_1 mode of S_n chains. The amplitude of these bands decreases slightly when the Ge/Sb ratio changes. This has to be related to the reduced number of S bonding with Sb. Furthermore, when the Ge/Sb ratio decreases, the amplitude of the shoulder at 300 cm^{-1} increases and the main band becomes broader indicating that the number of GeS_4 units decreases in the glass network while the number of SbS_3 units increases. However, as seen in Table 1, the nonlinear refractive index increases when few Ge atoms which have no electronic lone pair are replaced by Sb atoms which possess one electronic lone pair indicating that the n_2 is related to the number of Sb–S bonds. This was confirmed by preparing glasses with different Ge/S ratios keeping the atomic percent of Sb ~7–9%. Indeed, as seen in Table 1, when the Ge/S ratio increases, the density, the glass transition temperature as well as the nonlinear refractive indices of these glasses increase. The absorption band-gap position shifts to higher wavelength. One can notice that the main band in the Raman spectra (Fig. 2b) becomes broader. The bands in the 450–500 cm^{-1} range, related to homopolar S–S bonds, disappear and new bands in ~200 and ~250 cm^{-1} appear indicating the presence of homopolar Ge–Ge bonds in agreement with [32]. It is clear that an increase of the Ge/S ratio decreases the number of homopolar S–S bonds leading to the formation of homopolar Ge–Ge bonds. This results in the absorption band-gap shifting to a higher wavelength and also in an increase of n_2, showing that n_2 is not related to the number of homopolar S–S bonds. These results confirm that n_2 depends on the number of heteropolar bonds such as Ge–S and Sb–S or homopolar Ge–Ge bonds.

New selenide glasses have also been investigated with different Ge/Se contents and their compositions are listed in Table 1. The T_g and the density increase when the Ge/Se ratio increases and the absorption band-gap position shifts to higher wavelength as seen in Fig. 3a. The Raman spectra of these new glasses are depicted in Fig. 3b. The Raman spectra, depending on the composition, exhibit a band at 200 cm^{-1} which has been attributed to A_1 vibrations of the corner-sharing $GeSe_{4/2}$ tetrahedra and the one at 215 cm^{-1} to A_1^c breathing vibration of edge-sharing $Ge_2Se_{8/2}$ bi-tetrahedra in accordance with Murase [33]. The shoulder at 190 cm^{-1} has been attributed to heteropolar Sb–Se bond vibrations in the $SbSe_{3/2}$ pyramids [34]. The band at 250 cm^{-1} with a shoulder at 266 cm^{-1}, has an intensity that increases with the progressive introduction of Se, corresponding to A_1 modes of vibration of Se, in rings and in chains, respectively, in good agreement with the Raman spectrum of $GeSe_2$ [35]. When the Se content decreases compared to the Ge content, there is a progressive decrease of the amplitude of the bands located in the range 250–270 cm^{-1} as compared to the intensity of the large band at 200 cm^{-1} showing a decrease of the homopolar Se–Se bonds in rings and in chains. This is in agreement with the apparition of the shoulder at 180 cm^{-1} for lower concentration of Se. Indeed, this shoulder was assigned to vibrations of $Ge_2Se_{6/2}$ structural units with Ge–Ge bonds [36]. Moreover, the intensity of the shoulder at 215 cm^{-1} increases dramatically indicating that the structure of the low Se concentrated glass is formed by a larger number of $Ge_2Se_{8/2}$ and $Ge_2Se_{6/2}$ units in the glass network due to the low content of Se. This change of the structure results in a lower n_2 as seen in Table 1. This confirms that n_2 in the Ge–Sb–Se network cannot be related to the presence of

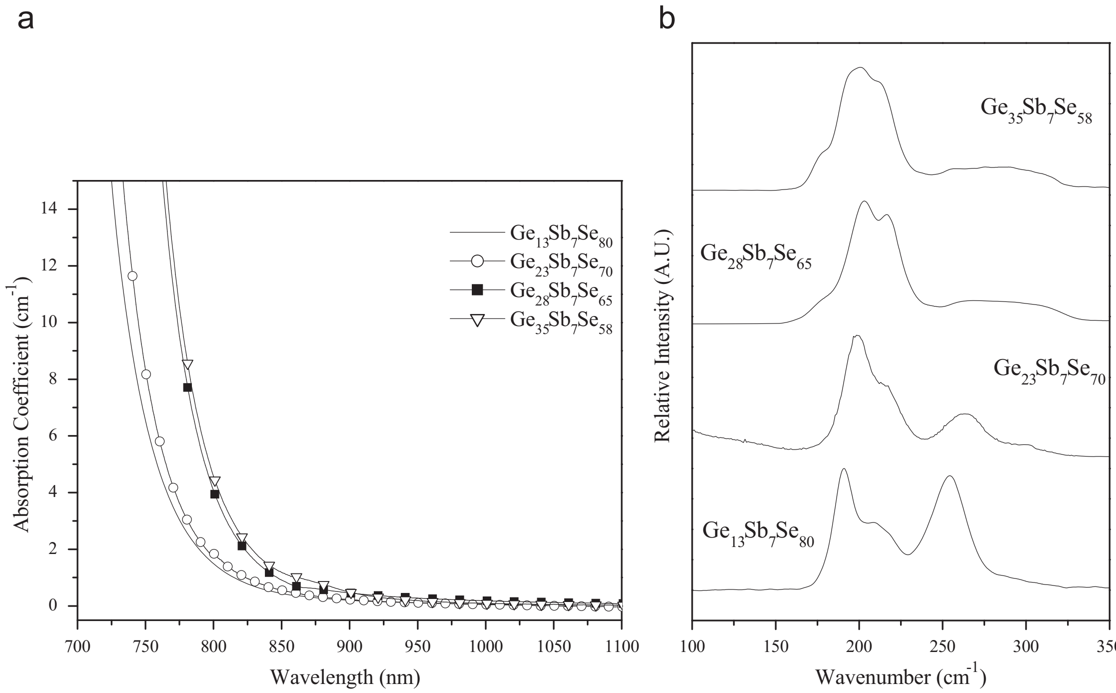

Fig. 3. (a) Absorption and (b) Raman spectra of the selenide glasses with different Ge/Se ratios.

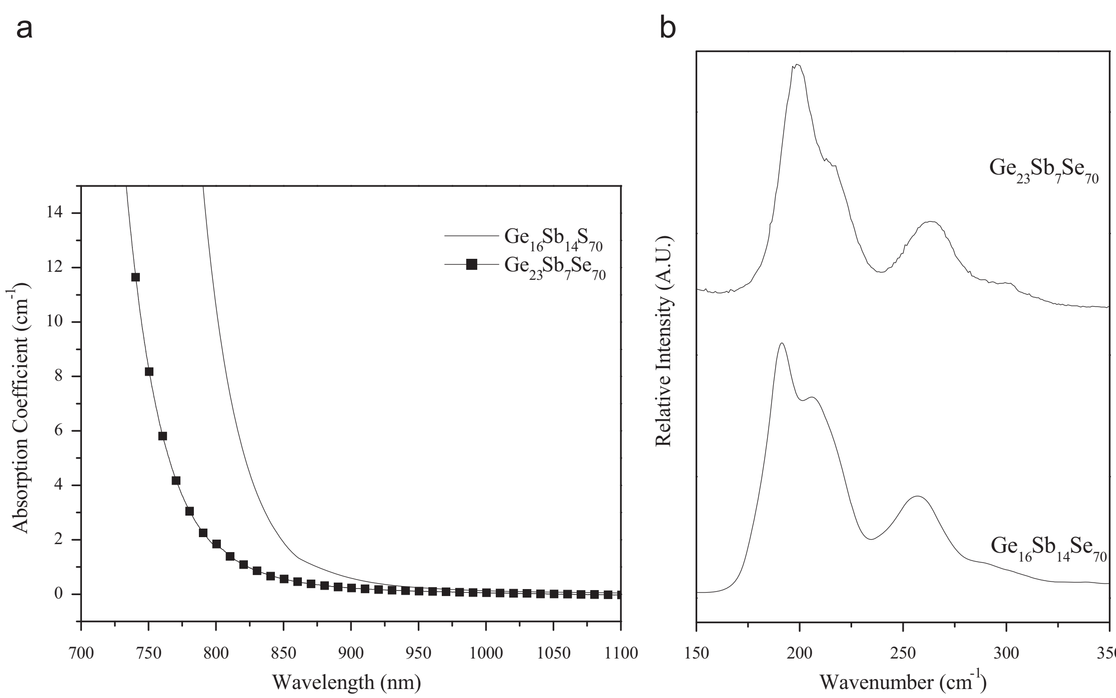

Fig. 4. (a) Absorption and (b) Raman spectra of the selenide glasses with different Ge/Sb ratios.

homopolar Se–Se bonds. As seen in Table 1 and in Fig. 4a, a decrease of the Ge/Sb ratio shifts the absorption band gap to a higher wavelength, decreases the T_g while the density and the nonlinear refractive index increase. Fig. 4b shows the Raman spectra of these glasses. When the Ge/Sb ratio decreases, the main band in the range 175–225 cm^{-1} becomes broader and shifts slightly to lower wavenumber. As explained above, this indicates that a decrease of the Ge/Sb ratio induces an increase of the $SbSe_3$ units and a decrease of $GeSe_{4/2}$ tetrahedra, as expected. Moreover, the amplitude of the shoulder at $\sim$215 cm^{-1} decreases strongly compared to the intensity of the band at $\sim$200 cm^{-1} showing that the introduction of Sb in higher content leads to the formation of edge-sharing $Ge_2Se_{8/2}$ bi-tetrahedra with a reduction of the number of corner-sharing $GeSe_{4/2}$ in the glass network. From these observations, the increase of the n_2 when the Ge/Sb ratio decreases for constant Se content confirmed that the n_2 is related to the number of heteropolar bonds in the glass network. In agreement with the evolution of the n_2 in the sulfide glasses, it is confirmed that n_2 is influenced more by an increase of Sb–Se bonds than by an increase of Ge–Se bonds.

4. Conclusion

The nonlinear refractive indices (n_2) and absorption (β) of new germanium-based sulfide and selenide glasses have been measured using modified Z-Scan technique at 1064 nm. We have confirmed that the n_2 is related to the number of heteropolar bonds Ge–S(Se) and Sb–S(Se) and is directly correlated to normalized photon energy while showing no connection to lone pair electron concentration alone. With exception of the glasses with the composition $Ge_{16}Sb_{14}S_{70}$ and $Ge_{31}Sb_9S_{60}$, the figure of merit (F) for the studied glasses are all >1 suggesting the glasses would not be suitable candidates for optical switching at 1064 nm but could be good candidates for applications at telecommunication wavelengths (1.55 μm) or beyond.

References

[1] C. Meneghini, A. Villeneuve, As_2S_3 photosensitivity by two-photon self-written channel waveguides, J. Opt. Soc. Am. B 15 (1998) 2946–2950.

[2] R. Rangel Rojoa, T. Kosa, E. Hajto, P.J.S. Ewen, A.E. Owen, A.K. Kar, B.S. Wherrett, Near-infrared optical nonlinearities in amorphous chalcogenides, Opt. Commun. 109 (1994) 145–150.

[3] T. Cardinal, K.A. Richardson, H. Shim, A. Schulte, R. Beatty, K. Le Foulgoc, C. Meneghini, J.F. Viens, A. Villeneuve, Non-linear optical properties of chalcogenide glasses in the system As–S–Se, J. Non-Cryst. Solids 256–257 (1999) 353–360.

[4] G.I. Stegeman, in: H.S. Nalwa, S. Myata (Eds.), Nonlinear Optics of Organic Molecules and Polymers, CRC Press, Boca Raton, 1997, pp. 799–812.

[5] C. Lopez, Evaluation of photo-induced structural mechanisms in chalcogenide glass, Ph.D. Thesis, College of Optics and Photonics at the University of Central Florida, 2004.

[6] H. Nasu, K. Kubodera, M. Kobayashi, M. Nakamura, K. Kamiya, Third-harmonic generation from some chalcogenide glasses, J. Am. Ceram. Soc. 73 (1990) 1794–1796.

[7] G. Lenz, J. Zimmermann, T. Katsufuji, M.E. Lines, H.Y. Hwang, S. Spälter, R.E. Slusher, S.-W. Cheong, J.S. Sanghera, I.D. Aggarwal, Large Kerr effect in bulk Se-based chalcogenide glasses, Opt. Lett. 25 (2000) 254–256.

[8] S. Chu, F. Li, H. Tao, H. Yang, S. Wang, C. Lin, X. Zhao, Q. Gong, SbS_3 enhanced ultrafast third-order optical nonlinearities of Ge–S chalcogenide glasses at 820 nm, Opt. Mater. 31 (2008) 193–195.

[9] P. Houizot, F. Smektala, V. Couderc, J. Troles, L. Grossard, Selenide glass single mode optical fiber for nonlinear optics, Opt. Mater. 29 (2007) 651–656.

[10] M. Guignard, V. Nazabal, A. Moreac, S. Cherukulappurath, G. Boudebs, H. Zeghlache, G. Martinelli, Y. Quiquempois, F. Smektala, J.-L. Adam, Optical and structural properties of new chalcohalide glasses, J. Non-Cryst. Solids 354 (2008) 1322–1326.

[11] J.S. Sanghera, J. Heo, J.D. Mackenzie, Chalcohalide glasses, J. Non-Cryst. Solids 103 (1988) 155–178.

[12] H. Guo, H. Tao, S. Gu, X. Zheng, Y. Zhai, S. Chu, X. Zhao, S. Wang, Q. Gong, Third- and second-order optical nonlinearity of Ge–Ga–S–PbI_2 chalcohalide glasses, J. Sol. State Chem. 180 (2007) 240–248.

[13] X. Yinsheng, Z. Huidan, Y. Guang, C. Guorong, Z. Qiming, X. Lei, Third-order nonlinearities in $GeSe_2$–In_2Se_3–CsI glasses for telecommunications applications, Opt. Mater. 31 (2008) 75–78.

[14] J.M. Harbold, F.O. Ilday, F.W. Wise, B.G. Aitken, Highly nonlinear Ge–As–Se and Ge–As–S–Se glasses for all-optical switching, IEEE Photon. Technol. Lett. 14 (6) (2002) 822–824.

[15] J.S. Sanghera, C.M. Florea, L.B. Shaw, P. Pureza, V.Q. Nguyen, M. Bashkansky, Z. Dutton, I.D. Aggarwal, Non-linear properties of chalcogenide glasses and fibers, J. Non-Cryst. Solids 354 (2008) 462–467.

[16] C. Rivero, K. Richardson, R. Stegeman, G. Stegeman, T. Cardinal, E. Fargin, M. Couzi, V. Rodriguez, Quantifying Raman gain coefficients in tellurite glasses, J. Non-Cryst. Solids 345 and 346 (2004) 396–401.

[17] C. Rivero, K. Richardson, R. Stegeman, G. Stegeman, T. Cardinal, E. Fargin, M. Couzi, Characterization of the performance parameters of some new broadband glasses for Raman amplification, Glass Technol. 46 (2) (2005) 80–84.

[18] M.D. O'Donnell, A.B. Seddon, D. Furniss, V.K. Tikhomirov, C. Rivero, M. Ramme, R. Stegeman, G. Stegeman, K. Richardson, R. Stolen, M. Couzi, T. Cardinal, Raman gain of selected tellurite glasses for high power IR fiber lasers calculated from spontaneous scattering spectra, J. Am. Ceram. Soc. 90 (5) (2007) 1448–1457.

[19] R. Stegeman, G. Stegeman, P. Delfyett Jr., L. Petit, N. Carlie, K. Richardson, M. Couzi, Raman gain measurements and photo induced transmission effects of germanium and arsenic based chalcogenide glasses, Opt. Exp. 14 (24) (2006) 11702–11708.

[20] L. Petit, A. Humeau, N. Carlie, G. Boudebs, H. Jain, A. Miller, K. Richardson, Correlation between the nonlinear refractive index and structure of germanium-based chalcogenide glasses, Mater. Res. Bull. 42 (2007) 2107–2116.

[21] M. Sheik-Bahae, A.A. Said, T.H. Wei, D. Hagan, E.W. Van Stryland, Sensitive measurement of optical nonlinearities using a single beam, IEEE J. Quant. Electron. 26 (1990) 760–769.

[22] Y. Cao, Q. Nie, S. Dai, X. Wang, Investigation of third-order nonlinear optical properties of Ge–Sb–S–Se chalcogenide glass, Acta Photon. Sin. 37 (2008) 203–206.

[23] L.A. Gomez, C.B. de Araujo, R. Putvinskis Jr., S.H. Messaddeq, Y. Ledemi, Y. Messaddeq, Nonlinear optical properties of antimony germanium sulfur glasses at 1560 nm, Appl. Phys. B 94 (2009) 499–502.

[24] M. Sheik-Bahae, D.J. Hagan, E.W. Van Stryland, Dispersion and band gap scaling of the electronic Kerr effect in solids associated with two-photon absorption, Phys. Rev. Lett. 65 (1990) 96–99.

[25] K. Tanaka, Nonlinear optics in glass: how can we analyze, J. Phys. Chem. Solids 68 (2007) 896–900.

[26] L. Petit, A. Humeau, N. Carlie, S. Cherukulappurath, G. Boudebs, K. Richardson, Non-linear optical properties of chalcogenide glasses in the glass system Ge/Ga–Sb–S/Se, Opt. Lett. 31 (10) (2006) 1495–1497.

[27] C. Quemard, F. Smektala, V. Couderc, A. Barthelemy, J. Lucas, Chalcogenide glasses with high nonlinear optical properties for telecommunications, J. Phys. Chem. Solids 62 (2001) 1435–1440.

[28] L. Petit, N. Carlie, K.C. Richardson, M. Couzi, F. Adamietz, V. Rodriguez, Correlation between physical, optical and structural properties of sulfide glasses in the system Ge–Sb–S, Mater. Chem. Phys. 97 (2006) 64–70.

[29] C. Julien, S. Barnier, M. Massot, N. Chbani, X. Cai, A.M. Loireau-Lozac'h, M. Guittard, Raman and infrared spectroscopic studies of Ge–Ga–Ag sulphide glasses, Mater. Sci. Eng. B 22 (1994) 191–200.

[30] Q. Mei, J. Saienga, J. Schrooten, B. Meyer, S.W. Martin, Preparation and characterization of glasses in the Ag_2S+B_2S_3+GeS_2 system, J. Non-Cryst. Solids 324 (2003) 264–276.

[31] B. Frumarova, P. Nemec, M. Frumar, J. Oswald, M. Vleck, Synthesis and optical properties of the Ge–Sb–S:$PrCl_{13}$ glass system, J. Non-Cryst. Solids 256–257 (1999) 266–270.

[32] V. Nazabal, P. Nemec, J. Jedelsky, C. Deverger, J. Le Person, J.L. Adam, M. Frumar, Dysprosium doped amorphous chalcogenide films prepared by pulsed laser deposition, Opt. Mater. 29 (2006) 273–278.

[33] K. Murase, in: P. Boolchand (Ed.), Insulating and Semiconducting Glasses, World Scientific Press, Singapore, 2000.

[34] Z.G. Ivanova, V. Pamukchieva, M. Vleck, On the structural phase transformations in $Ge_xSb_{40-x}Se_{60}$ glasses, J. Non-Cryst. Solids 293 and 295 (2001) 580–585.

[35] K. Jackson, A. Briley, S. Grossman, D.V. Porezag, M.R. Pederson, Raman-active modes of a-$GeSe_2$ and a-GeS_2: a first-principles study, Phys. Rev. B 60 (22) (1999) 14985–14989.

[36] K. Murase, T. Fukunaga, Y. Tanaka, K. Yakushiji, I. Yunoki, Investigation of large molecular fragments in glassy Ge_{1-x} (Se or S), Physica B 117 and 118 (1983) 962–964.